Ionization and positronium formation in noble gases

J. P. Marler, J. P. Sullivan,* and C. M. Surko
Department of Physics, University of California, San Diego, 9500 Gilman Drive, La Jolla, California 92093-0319, USA
(Received 14 October 2004; published 2 February 2005)

Absolute measurements are presented for the positron-impact cross sections for direct ionization and positronium formation of noble gas atoms in the range of energies from threshold to 90 eV. The experiment uses a cold, trap-based positron beam and the technique of studying positron scattering in a strong magnetic field. The current data show generally good, quantitative agreement with previous measurements taken using a qualitatively different method. However, significant differences in the cross sections for both direct ionization and positronium formation are also observed. An analysis is presented that yields another, independent measurement of the direct ionization and positronium formation cross sections that is in agreement with the present, direct measurements to within ±10% for argon, krypton, and xenon. Comparison with available theoretical predictions yields good quantitative agreement for direct ionization cross sections, and qualitative agreement in the case of positronium formation.

DOI: 10.1103/PhysRevA.71.022701 PACS number(s): 34.85.+x, 34.50.−s, 34.50.Fa

I. INTRODUCTION

Positron interactions with matter play important roles in many physical processes of interest. Examples include the origin of astrophysical sources of annihilation radiation, the use of positrons in medicine (e.g., positron emission tomography); the characterization of materials; and the formation of antihydrogen, which is the simplest form of stable, neutral antimatter. While the interactions of positrons with atomic targets have been studied for decades [1–3], many fundamental questions remain open [4]. This area is much less advanced, as compared, for example, with study of electron scattering processes, particularly at low energies. The reason for this is twofold. From an experimental viewpoint, positrons are much less common than electrons, and consequently techniques for using them to study scattering are less well developed. From a theoretical viewpoint, positron interactions with atoms and molecules are different in fundamental respects. In particular, the exchange interaction is absent, and an additional process, the formation of positronium, Ps (i.e., the "atom" which consists of an electron and a positron), is believed to play an important role, either as an open or closed channel.

Since there is no analog of positronium formation in electron scattering, the extensive understanding of electron interactions with atomic targets is of little help in developing procedures to treat this phenomenon theoretically. In particular, positronium formation requires the inclusion of an additional set of final states. This poses a serious challenge to theory that has not yet been solved, particularly at lower values of positron energy where simple perturbative approaches, such as the Born approximation, are invalid.

Positrons can ionize atoms and molecules through three processes, direct ionization,

$$A + e^+ \rightarrow A^+ + e^+ + e^-; \tag{1}$$

positronium formation,

$$A + e^+ \rightarrow A^+ + \mathrm{Ps}; \tag{2}$$

and direct annihilation,

$$A + e^+ \rightarrow A^+ + 2\gamma. \tag{3}$$

The first two processes have cross sections on the order of a_0^2, where a_0 is the Bohr radius, whereas the latter has a cross section that is orders of magnitude smaller [3]. Thus, to a good approximation,

$$\sigma_{TI} = \sigma_I + \sigma_{\mathrm{Ps}}, \tag{4}$$

where σ_T is the total ionization cross section, σ_I is the direct ionization cross section, and σ_{Ps} is the positronium cross section.

In this paper, we describe absolute measurements of positron-impact ionization and positronium formation in noble gases. While previous measurements of positron-impact direct-ionization cross sections in noble gases are in reasonable agreement [5–7], there are significant discrepancies in previous measurements of the corresponding positronium formation cross sections [8–15]. This lack of agreement has recently been discussed by Laricchia *et al.*, and is illustrated in Fig. 1 [16]. One goal of the present work is improvement in the accuracy of these positronium formation cross sections.

The measurements presented here are made with a cold, trap-based positron beam. Scattering is studied in a strong magnetic field, which permits absolute measurements of the scattering cross sections without need for normalization to other cross sections. Measurements are presented for direct ionization and positronium formation in the noble gases, neon, argon, krypton, and xenon. These targets are chosen because of their relatively simple atomic structure and the fact that they occur naturally as single atoms. Helium was not studied for technical reasons. We compare the results of the experiments with other available measurements for these processes and available theoretical predictions.

Absolute comparison is made with the most complete, recent sets of experimental measurements of these processes

*Present address: RSPhysSE, Australian National University, Canberra, Australia.

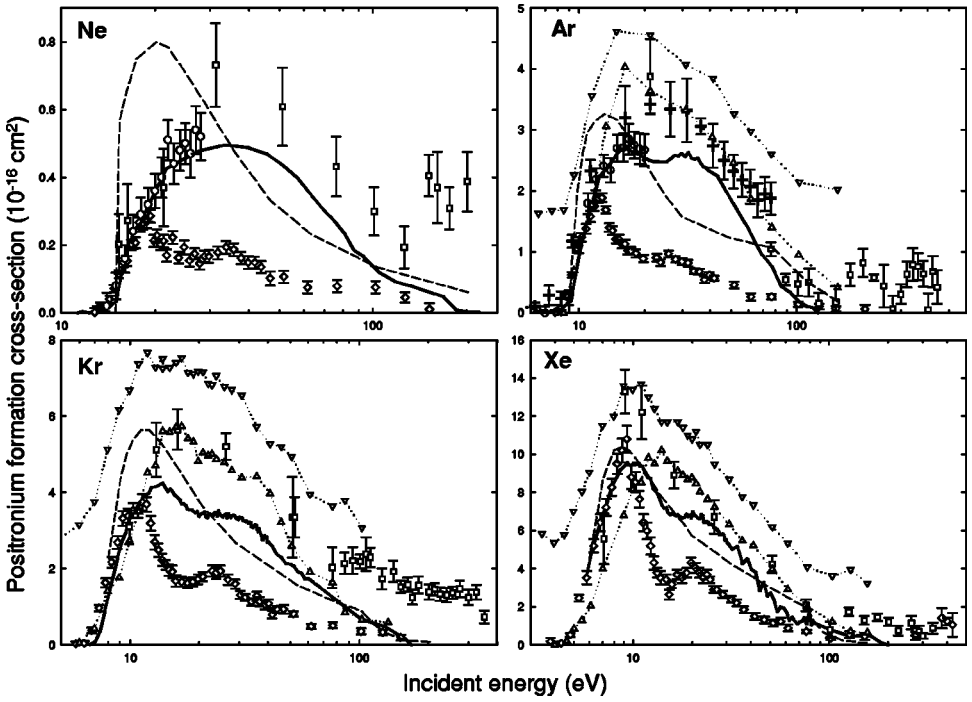

FIG. 1. Summary of previous positronium formation cross section measurements for neon, argon, krypton, and xenon as a function of positron energy: Figure and (—) are from Ref. [16]; (◇) [8]; (○) [9]; (□) [12–15]; (+) [10]; (▽) and (△), upper and lower limits from Ref. [11]; and (- -) theory of Ref. [17].

using different techniques [5,7,16]. These comparisons indicate good quantitative agreement, but also indicate some discrepancies. The present measurements of direct ionization cross sections are ~15–30% larger than the previous measurements. The positronium formation cross sections agree well with the most recent measurements below the direct ionization threshold, but in some cases are lower at high energy (i.e., argon and krypton). An analysis is presented that indicates a possible origin of these discrepancies. Based upon this analysis, we arrive at two independent data sets for the positronium formation cross sections in argon, krypton, and xenon that agree in absolute value to better than ±5–10% in the range of energies from threshold to several tens of electron volts. In the case of neon, while there is reasonable absolute agreement between the experiments, more significant discrepancies remain (e.g., at the ±15% level).

Comparison of the measured direct ionization cross sections with available theoretical calculations yields quantitative agreement at the 20% level. Comparison of the measured positronium formation cross sections with available theoretical predictions yields fair qualitative agreement. However, the lack of quantitative agreement between theory and experiment highlights the need for further consideration of this important and fundamental process.

II. EXPERIMENTAL TECHNIQUES

A. Trap-based positron beam

The experimental technique for forming a cold, trap-based positron beam has been described in detail [18,19]. Positrons emitted from a ^{22}Na radioactive source are slowed to electron volt energies by interaction with a frozen neon moderator. They are then guided magnetically to a three-stage buffer-gas Penning-Malmberg trap where the magnetic field is 0.15 T. The positrons are trapped and cooled by inelastic collisions with a dilute gas mixture of N_2 and CF_4 ($p=5\times10^{-7}$ torr in the third stage of the trap). Using this technique, the positrons cool to the temperature of the surrounding electrodes (i.e., 300 K≡25 meV) in ~0.1 s.

The process of positron beam formation is illustrated schematically in Fig. 2. Following a cycle of positron trapping and cooling, the electric potential in the accumulator is carefully raised to force the positrons out of the trap at a well defined energy, set by the potential V in Fig. 2. The positron beam energy in the gas cell, $\epsilon=e(V-V_C)$, where V_C is the potential of the cell, can be varied from ~0.05 to 100 eV. Differential pumping isolates the buffer-gas trap from the scattering experiment beamline.

The positron pulse is then passed through the scattering cell which contains the test gas. Positrons that have not annihilated or formed positronium in the scattering cell are guided by the magnetic field through a cylindrical retarding potential analyzer (RPA) electrode, and finally to a metal detector plate where the positrons annihilate. The magnetic field in the gas cell is 0.09 T. The magnetic field in the RPA is adjustable from zero to 0.09 T. The resulting annihilation

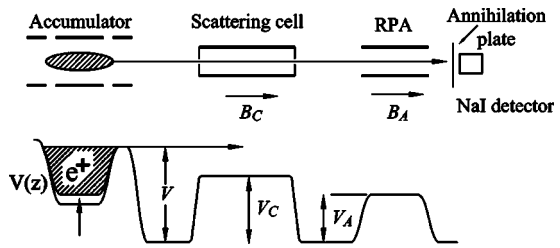

FIG. 2. Schematic diagram of the electrode structure (above) and the electric potentials (below) used to study scattering with a trap-based positron beam.

gamma rays from the detector plate are monitored using an NaI crystal and photomultiplier.

The gas cell is 38.1 cm long and 7.0 cm in diameter, with entrance and exit apertures 0.5 cm in diameter. Cylindrical mesh grids inside the cell at the entrance and exit are used to further tune the potential to be constant near the entrance and exit of the cell. The electrical potential V_A on the RPA can be varied to analyze the energy distribution of the positrons that pass through the scattering cell. The RPA is also used to analyze the incident energy distribution of the positron beam (i.e., with the test gas removed from the scattering cell). The energy resolution of the positron beam used in the experiments described here is $\sim$25 meV (full width at half maximum).

The base pressure of the scattering apparatus is $\sim 5 \times 10^{-8}$ torr. The apparatus achieves this vacuum environment by the use of cryopumps. These pumps do not work with helium nor as well with neon as with the heavier noble gases. As a consequence, run time on neon is limited, resulting in larger uncertainties for these data.

B. Measuring integral scattering cross sections in a strong magnetic field

The ionization and positronium formation cross-section measurements presented here were done using a technique that relies on the fact that the positron orbits are strongly magnetized [20,21]. In a strong magnetic field, where the positron's gyroradius is small compared to the characteristic dimensions of the scattering apparatus (but still large compared to atomic dimensions), the total kinetic energy is separable into two components: kinetic energy in motion parallel to the magnetic field, $E_\parallel$, and the energy in the cyclotron motion in the direction perpendicular to the field, $E_\perp$. For the experiments described here, the magnetic field in the scattering region, B_C, and in the analyzing region, B_A, can be adjusted independently. This then allows us to take advantage of the adiabatic invariant, $\xi = E_\perp / B$. To a good approximation, ξ is constant in the case relevant here, namely when the magnetic field is strong in the sense described above, and the field varies slowly compared to a cyclotron period in the frame of the moving positron.

Initially, the positron energy is mainly in the parallel direction (i.e., $E_\perp \sim 0.025$ eV $\ll E_\parallel$). If a positron is scattered in the gas cell, then some of the positron's initial energy will be transferred from the parallel to the perpendicular component, with the specific amount depending on the scattering angle. The RPA measures only the final $E_\parallel$ distribution of the positrons. Thus when only elastic scattering is present (i.e., the total kinetic energy of the positron is conserved), this energy distribution can be used to determine the differential elastic scattering cross section [21]. However, when inelastic processes are present the positron's total kinetic energy is not conserved. In this case, the observed loss in $E_\parallel$ is the result of both a decrease in total kinetic energy and a redistribution of energy into $E_\perp$.

The integral cross section measurements reported here rely on the fact that, by reducing the magnetic field in the analyzing region, most of the energy in $E_\perp$ can be transferred back into $E_\parallel$ (due to the fact that ξ is constant), while the total kinetic energy of the positron remains constant. In the current experiments, the magnetic field ratio between the scattering cell and RPA is 35:1, which is sufficient to ensure that the value of $E_\parallel$ at the RPA is approximately equal to the total kinetic energy of the positron at that location. Thus the difference between the incident positron energy and that measured by the RPA is an absolute measure of the energy lost due to inelastic scattering. While information about angular scattering is lost, this procedure provides an accurate method with which to make integral inelastic cross-section measurements [22,23]. In particular, as described in more detail below, this technique provides absolute cross-section measurements by normalizing the transmitted signal to the incident beam strength. In the experiments reported here, the incident energy of the positrons was varied from below the thresholds for positronium formation (and ionization) to 90 eV.

C. Direct ionization

For direct ionization measurements, the RPA is set to exclude positrons that have lost an amount of energy corresponding to the ionization energy or greater. As a result, only positrons that have lost less than this amount of energy pass through the RPA to the detector. The difference between the signal strength when the RPA is set to allow all of the positrons to pass through the RPA and that when the RPA is set to reject those that have ionized the test species is denoted as I_I.

The incident beam strength I_0 is measured by ensuring that the positron energy inside the gas cell is below the threshold for positronium formation (i.e., the ionization energy minus the positronium binding energy, 6.8 eV). This measurement is taken with the test gas in the scattering cell. Modeling has demonstrated that scattering near 90° (which would also appear as a loss from the beam) is small compared to positronium formation [21]. Positrons that backscatter in the cell are reflected from the back wall of the trap and sent back toward the detector.

The absolute, direct ionization cross section is then given by the equation

$$\sigma_I(\epsilon) = \frac{1}{n_m l} \frac{I_I(\epsilon)}{I_0}, \tag{5}$$

where $I_I(\epsilon)$, as defined previously, is the magnitude of the loss in signal strength due to ionization by positrons with energy ϵ in the gas cell, n_m is the number density of the target gas, and l is the path length. In Eq. (5) and elsewhere in this paper, we assume the weak-scattering limit of the Lambert-Beer law, namely that the fraction of scattered particles $\Delta I \ll I_0$.

Test gas pressure is measured using a capacitance manometer with an expected error of $<1\%$. The apertures on the gas cell are sufficiently small so there is a well defined interaction region where the pressure and the potential are constant, and therefore the path length can be accurately determined. Equation (5) is then used to determine the absolute cross section for ionization. The main source of noise is statistical.

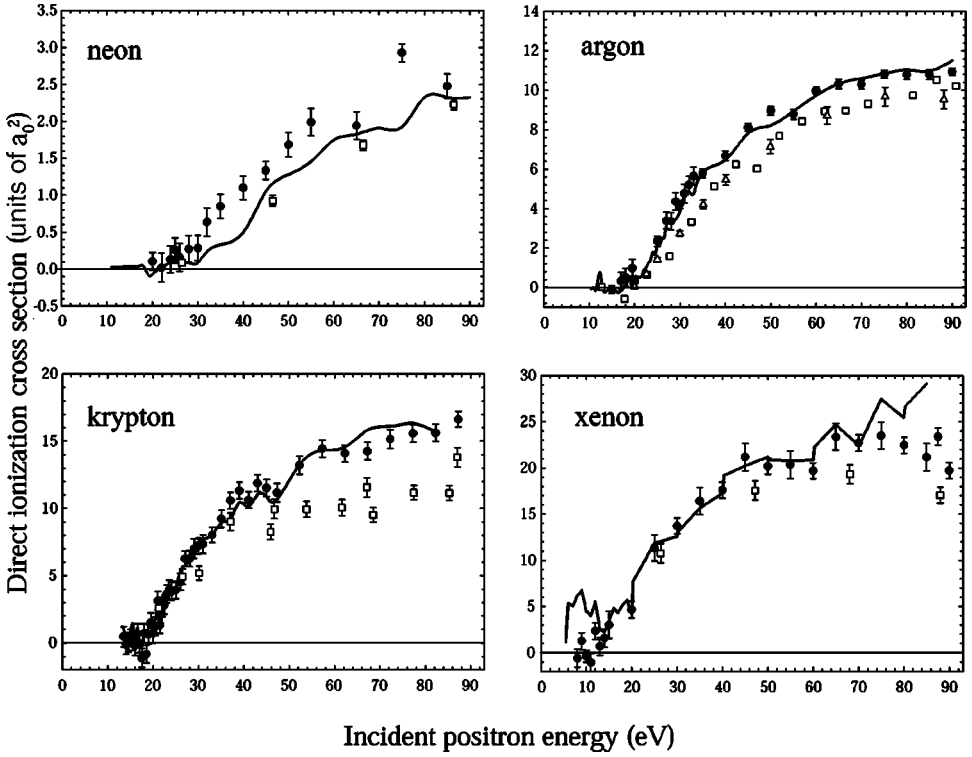

FIG. 3. Direct ionization cross sections (●) as a function of positron energy for neon, argon, krypton, and xenon. These data are compared with two other determinations of these cross sections: (□) the direct ionization measurements from Refs. [5,7]; and (—) using the total ionization from Ref. [16] minus the present measurements for the positronium formation. Also shown for comparison in argon are (△) the experimental data from Ref. [6].

The total cross section for each target atom was measured in order to determine the appropriate operating pressure. The pressure was chosen such that the probability of undergoing a single collision in the scattering cell was less than 15%. This corresponded to target gas pressures in the range of 0.05–0.5 millitorr for the target species studied.

D. Positronium formation

Since positronium is a neutral atom, positrons that form positronium in the scattering cell will not be guided by the magnetic field, and the vast majority are therefore lost before striking the detector. Positronium lifetime aside, the solid angle $\delta\Omega$ of the annihilation plate as viewed from the gas cell through the exit aperture of the cell is negligibly small, $\delta\Omega < 10^{-3}$. Positrons will either annihilate in the scattering cell because of the short annihilation lifetime of the Ps atom (i.e., 0.12 ns for parapositronium and 142 ns for orthopositronium), or drift out of the beam and annihilate at the walls of the cell. In either case, positronium formation results in a loss of positron beam current. All positrons that do not form positronium will be transmitted through the RPA (which is grounded during these measurements) and strike the detector plate.

The difference between I_0 and the transmitted beam strength when the positron has energy ϵ in the gas cell is denoted as $I_{\mathrm{Ps}}(\epsilon)$ and is proportional to the number of positronium formed at that energy. The only other possible positron loss process is so-called direct annihilation. Since the cross section for direct annihilation at the energies studied is orders of magnitude smaller than that for positronium formation, this contribution is neglected.

Therefore the positronium formation cross section is

$$\sigma_{\mathrm{Ps}}(\epsilon) = \frac{1}{n_m l}\frac{I_{\mathrm{Ps}}(\epsilon)}{I_0}, \tag{6}$$

where n_m and l are defined above. I_0 is again the incident beam strength measured with gas in the cell with the positron energy in the cell less than the threshold for positronium formation.

III. RESULTS AND ANALYSIS

A. Direct ionization

Shown in Fig. 3 are measurements of the direct ionization cross sections made using the techniques described above. The cross sections in this figure and the following figures in this paper are given in units of a_0^2, where a_0 is the Bohr radius. For the present data in this paper, the error bars shown in Fig. 3 and the following figures are those due to counting statistics. Systematic errors in the pressure and path length measurements are estimated to be $\leqslant 2\%$. The direct ionization data in Fig. 3, are compared with the experimental results of Refs. [5,7] renormalized as described in Ref. [16]. A third determination of these cross sections (solid lines in Fig. 3) is discussed in Sec. III C below. The data from Refs. [5,7] are derived from relative cross-section measurements made in a crossed beam experiment by recording the coincidences between ions collected and positrons detected after the positrons passed through the interaction region. The absolute values of the cross sections were determined by normalization to the analogous electron cross sections at higher energies, where both cross sections are predicted to be the same, and the absolute values of the electron cross sections are known.

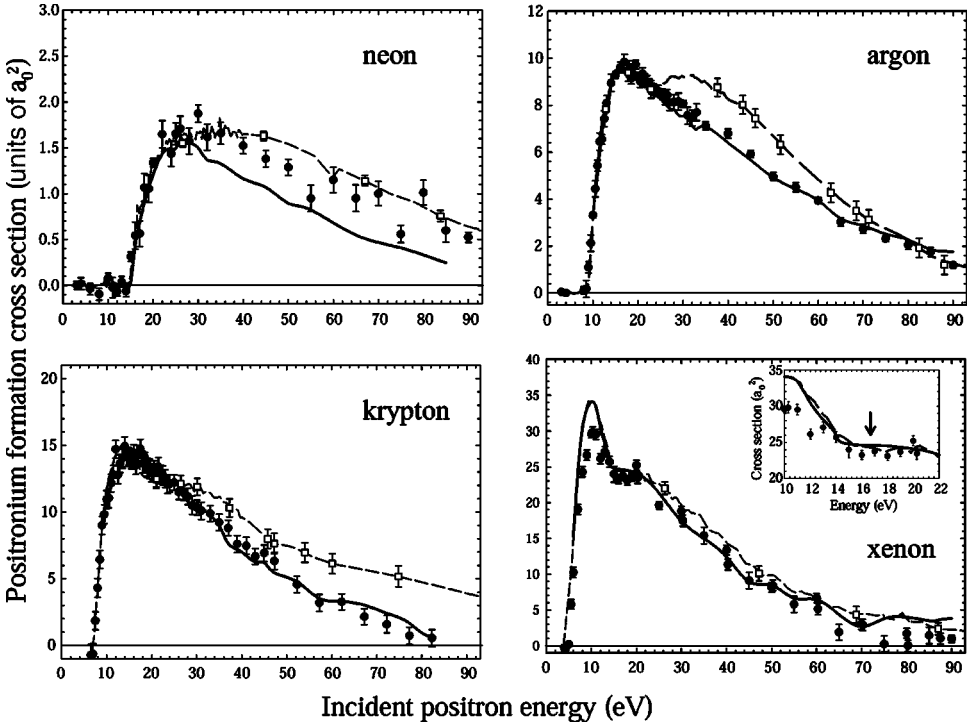

FIG. 4. The present direct measurements (●) of the positronium formation cross sections for neon, argon, krypton, and xenon as a function of incident positron energy. These data are compared with two other determinations of these cross sections: (- - □ - -) the method of Ref. [16] using the total ionization of Ref. [16] minus the direct ionization measurements from Refs. [5,7]; (—) using the total ionization from Ref. [16] minus the present measurements for the direct ionization. The inset shows the "shoulder" in xenon on an expanded energy scale. See text for details.

The two data sets shown in Fig. 3 agree reasonably well. The only qualitative difference is that, generally, the measurements presented here are somewhat above those of previous measurements, from ~15% in argon and xenon to ~30% in krypton.

B. Positronium formation

The present measurements of positronium formation cross sections are shown in Fig. 4. The error bars represent counting statistics. The data are generally featureless, reaching a maximum and then decreasing monotonically at higher energies. The only exception is a possible shoulder in the data for xenon that is shown on an expanded scale in the inset. This feature is discussed below.

It is instructive to compare these measurements of the positronium formation cross sections with those of Ref. [16], which of all previous measurements best match the present data over the range of energies studied. The experiment of Ref. [16] was performed using a channeltron to count the number of ions produced when positrons interact with a gas jet in a crossed beam experiment. The ions are extracted from the interaction region using a small electric field. These measurements and the direct ionization cross-section measurements of Refs. [5,7], discussed above, were used to obtain positronium formation cross sections, which are equal to the difference between the total-ionization and direct-ionization cross sections [i.e., Eq. (4)]. By contrast, the positronium formation cross-section measurements in the present experiment are made directly. They do not depend on measurements of either direct or total ionization. The present measurements are also absolute and do not require further normalization in contrast to the procedures used in Ref. [16].

Szłuińska and Laricchia recently made another independent measurement of the positronium cross section in argon and xenon using a coincidence technique between ions and annihilation gamma rays [24]. These measurements are in good agreement with those of Ref. [16] at low values of positron energy. However, at higher values of positron energy (e.g., 40 eV in Ar and 16 eV in Xe), the most recent measurements are higher than those made earlier. The authors conjecture that this is due to the lack of confinement of their positron beam due to the modest values of magnetic field available. These measurements show the onset of a double-peaked structure similar to that reported in Ref. [16] and are not consistent with the measurements presented here. In principal, the second peaks in Ref. [24] might arise if the positron beam in this experiment began to be not well confined by the applied magnetic field of 130 G at energies comparable to the low-energy side of those peaks. In Ref. [24], Szłuińska and Laricchia indicate that they do not think this is the case.

The two sets of measurements of positronium formation cross sections shown in Fig. 4 are in fairly good, quantitative agreement. This is impressive considering that very different experimental techniques were used to make the measurements. There are, however, some systematic discrepancies. In neon, there is reasonably good agreement between the two sets of measurements. In argon, both sets of measurements match very well up to about 25 eV. The data from Ref. [16] have a second peak at about 32 eV. This feature is absent in the present measurements, that decrease monotonically at higher energies. As a result, the present measurements give a lower value for the cross sections from 25 eV to about 70 eV. In krypton as in argon, both experiments provide similar values of the cross section up to 25 eV, but the present measurements are lower at larger energies. In xenon, the agreement between the two experiments is good over the range of energies studied.

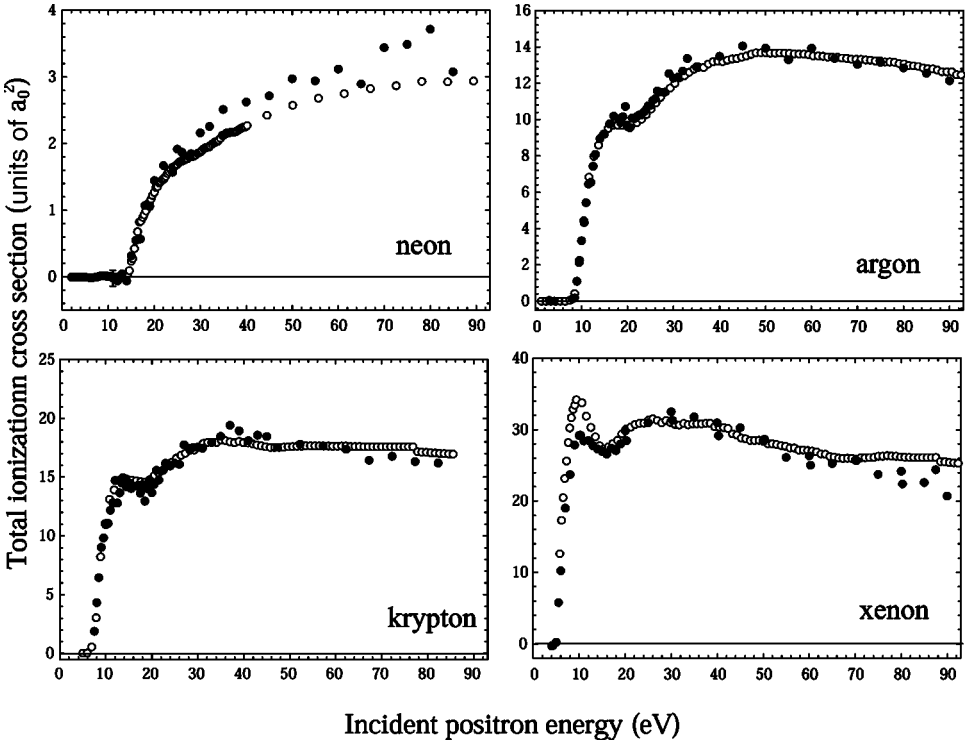

FIG. 5. The present measurements (●) of the total ionization cross section for neon, argon, krypton, and xenon. Also shown for comparison are (○) the analogous cross sections from Ref. [16].

Thus the major differences between the two sets of measurements are in argon and krypton at energies greater than the peak in the cross sections, which leads us to further consideration of the data. We note that the differences between the two measurements of positronium formation cross sections occur in the range of energies where direct ionization is appreciable. This quantity was used in Ref. [16], together with their total ionization measurements to obtain positronium formation cross sections.

The only qualitative feature of note in the present data beyond the main peaks in the cross sections is a shoulder observed in xenon in the approximate energy range, $15 \leqslant \epsilon \leqslant 20$ eV, and shown for clarity in the inset of the xenon plot in Fig. 4. While this is not far from the threshold for the formation of ground-state positronium with an inner-shell (5*s*) electron in xenon, $\epsilon_{\mathrm{th}} = 16.7$ eV (indicated by the arrow in the inset), the shoulder appears to start at a somewhat lower energy [25].

C. Total ionization and further analysis

As shown in Fig. 5, when the present, direct measurements of the direct ionization and positronium formation cross sections are combined using Eq. (4) to calculate the *total* ionization cross sections, the resulting total cross sections are, in fact, in good absolute agreement with those reported in Ref. [16]. The principal differences are that the current data have a somewhat higher cross section at higher energies in neon, and lower values at the initial peak in xenon.

Based on this observation and in order to explore further the differences in the two sets of measurements for the direct ionization and positronium formation cross sections, a calculation was performed which is similar in spirit to that in Ref. [16]. We use the total ionization cross-section measurements of Ref. [16], but instead of using their direct ionization cross section measurements, the direct ionization cross-section measurements from the present experiment are used. The results of this analysis are shown by the solid lines in Fig. 4. With the exception of neon, the cross sections obtained using this procedure agree well with the present, direct measurements.

The discrepancy between the solid lines and solid circles in Fig. 4 and the measurements from Ref. [16] (open squares) could be explained if there was an undercounting of ions in the direct ionization measurements reported in Ref. [16]. This hypothesis is consistent with the fact that the two sets of positronium formation cross-section measurements agree well in the region of energies where the direct ionization cross sections are comparatively small and differ where they are larger. Thus for argon, krypton, and xenon, there is excellent agreement over most of the range of energies studied between the two independent measurements of the positronium formation cross sections presented here (i.e., the solid circles and solid lines in Fig. 4.)

In order to investigate further the *direct* ionization cross sections, we followed a similar procedure to deduce the ionization cross sections from the results of our positronium formation cross sections (which are independent measurements from our direct ionization cross sections). We use Eq. (4) but this time subtract our positronium formation cross sections from the total ionization cross sections of Ref. [16] to obtain the direct ionization cross sections. The results of this analysis are shown as solid lines in Fig. 3. Although not surprising given the similarities between the total cross sections of Ref. [16] and the present work, there is excellent agreement between these two independent measurements of the direct ionization cross sections in the case of argon, krypton, and xenon.

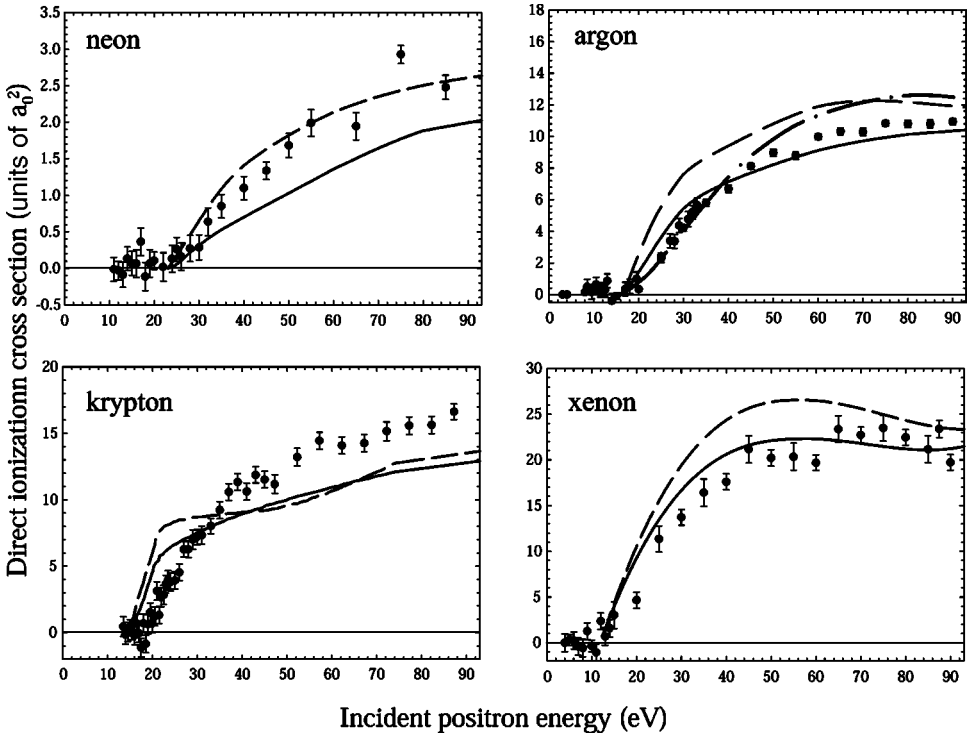

FIG. 6. Comparison of direct ionization cross sections (●) as a function of positron energy for neon, argon, krypton, and xenon with the theoretical predictions of (- -) CPE model of Refs. [26,28], (—) CPE4 model of Refs. [26,28], and (-··-) [29].

In neon, the two sets of measurements for both the positronium or direct ionization cross sections (i.e., Ref. [16] and the current measurements) agree reasonably well, and the results of our additional analysis does not yield better agreement with the present measurements for either of these cross sections. We note that we are less confident in our neon results due to the difficulty of cryopumping neon gas. Whether this is the origin of the remaining discrepancy is unclear.

With regard to the positronium formation cross sections in Fig. 4, the data sets shown by the solid circles and lines are in reasonably good absolute agreement with the previous measurements of Ref. [16], only differing in some details. They are in excellent agreement in xenon and good agreement in neon, with little or no qualitative trends to mention. In krypton, the present measurements are significantly lower at higher energies, e.g., $\epsilon \geqslant 30$ eV. A qualitative difference occurs in argon, where the data of Ref. [16] show a second peak in the cross section at energies beyond the main peak, i.e., at $\epsilon \sim 25$ eV. This feature, which in previous work [16] was tentatively attributed to the excitation of excited-state positronium, is not seen in the data and further analysis presented here.

IV. COMPARISON WITH THEORY

A. Direct ionization

In Fig. 6, we compare the direct ionization cross-section measurements presented here with available theoretical calculations. The dashed curves are the CPE (Coulomb plus plane waves) model of Refs. [26,27]. In this model, only the interaction of the positron and the ejected electron with the residual ion are considered. The solid lines in Fig. 6 are referred to by the authors as the CPE4 model. This more detailed model takes into account the fact that the ejected electron moves in the combined fields of the ion and the scattered positron. The assumptions for the scattered positron remain the same as in the CPE model. More recent calculations for the near-threshold cross sections using both the models are presented in Ref. [28]. In Fig. 6, the data from the near-threshold and the higher impact energies were combined to form the curves shown, with a bias toward the calculation at higher energies where the two calculations overlap.

Also shown in Fig. 6 are the results of a recent calculation by Bartschat [29]. This method is based upon the formalism outlined in Ref. [30] and the computer program described in Ref. [31]. The basic idea is to describe a "fast" projectile positron by a distorted wave and then calculate the initial bound state and the interaction between the residual ion and a "slow" ejected electron by an *R*-matrix (close-coupling) expansion. The results shown for argon in Fig. 6 were obtained using a first-order distorted-wave representation for the projectile and a two-state close-coupling approximation for electron scattering from Ar^+, coupling only the ionic ground state $(3s^2 3p^5)^2 P^o$ and the first excited state $(3s 3p^6)^2 S$. The ionic target description is the one used by Burke and Taylor [32] for the corresponding photoionization problem and then later by Bartschat and Burke [33] in the calculation of single-differential and total ionization cross sections of argon by electron impact.

In this calculation, the distortion potential for the positron was chosen as the static ground-state potential of neutral argon. Compared to pure distorted-wave models such as CPE and CPE4 mentioned above, the principal differences lie in the exact description of exchange effects between the ejected electron and the residual ion, the small amount of channel

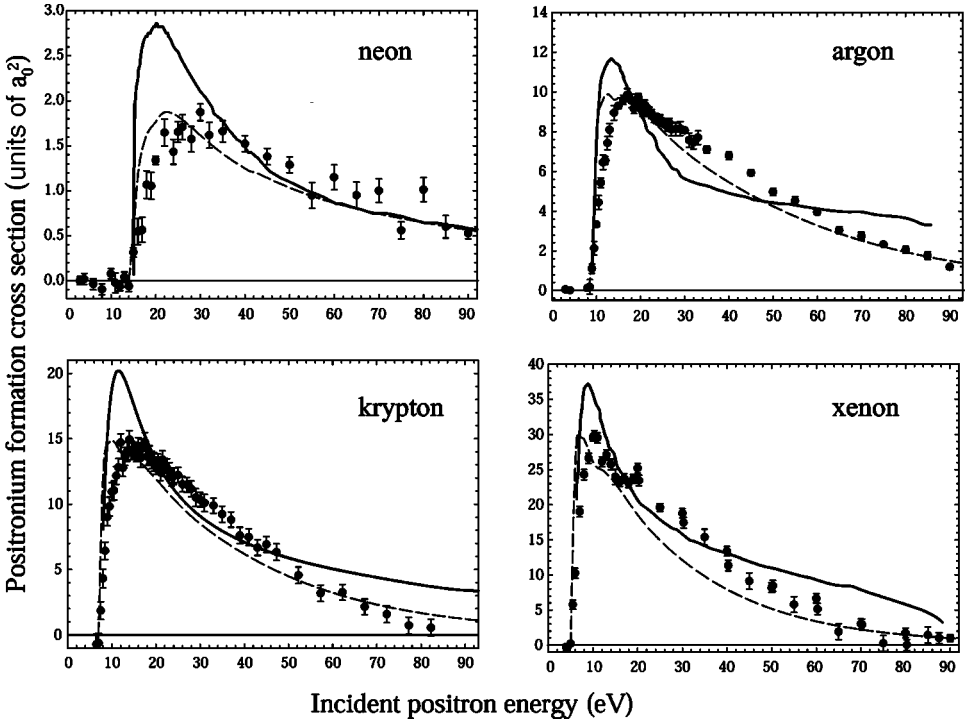

FIG. 7. Comparison of the present measurements (●) of the positronium formation cross section for neon, argon, krypton, and xenon with the theory of (—) Ref. [17]. Also shown is the theory of (- -) Ref. [35], scaled by factors of 0.61 (neon), 0.51 (argon), 0.37 (krypton), and 0.31 (xenon), so that the maximum values are equal to the maximum values of the experimental data.

coupling, and an accurate description of the ionic structure and the initial atomic bound state. On the other hand, this model does not account for any postcollision effects between the outgoing projectile and the ejected electron. Results for the other targets, as well as a detailed analysis regarding the sensitivity of the predictions on the details of this hybrid model, will be presented elsewhere [34].

The agreement between the measurements and theory is reasonably good. The agreement between the CPE and CPE4 calculations and the data varies from atom to atom and from one region of energy to another.

B. Positronium formation

In Fig. 7 the results of the present experiments are compared with the theoretical calculations of Refs. [17,35]. The earlier calculations [17] were performed using a coupled static-exchange approximation. Only positronium formation in the ground state was considered. The authors refer to this approximation as "truncated," because the exchange interaction between the Ps atom and the noble gas ion was neglected. With the exception of argon, only electron capture from the outer shell was included. In argon, electron capture from the next inner shell (3*s*) was also included. This contribution to the cross section was found to be small, and consequently, it was conjectured that this process likely amounted to a small contribution for the other atoms studied.

The second calculation was performed using the distorted-wave Born approximation (DWBA) [35]. While the authors do not consider this approximation to be the most appropriate approach at the energies of interest here, it was used because it is able to treat positronium formation in higher excited states. These calculations included capture from both the outer and next-inner shells of the atoms, however, the latter contribution is found to be small.

In all cases, the static exchange model [17] agrees fairly well with the absolute magnitudes of the maxima of the measured cross sections. However, the predicted dependences of the cross sections on positron energy are not in such good agreement with the measurements. The predictions rise too quickly near threshold, then fall more quickly than the data at energies larger than the peaks in the cross sections. Finally, with the exception of neon, the predicted values are larger than the measured cross sections at higher values of energy, $\epsilon \gtrsim 50$ eV.

In the case of the DWBA calculations [35], as shown in Fig. 7, a sizable scale factor (i.e., 0.31–0.61) is required to match the magnitudes of the measured cross sections. Even with the application of these scale factors, the predicted cross sections still rise more quickly than the data near threshold. Other than these discrepancies, the *shapes* of the predicted and measured cross sections as a function of incident positron energy are in reasonably good agreement. Neither of the calculations predict a second maximum similar to those reported in Ref. [16] and most pronounced in the argon data in that paper (cf., Fig. 4).

C. Total ionization

In Fig. 8, the experimental results of the total ionization cross section for argon are compared to the predications of a many-body theory calculation for the *total inelastic* cross section [36]. Experiment and theory agree reasonable well in shape and magnitude above 30 eV, but differ more significantly at lower energies. The theoretical calculation includes not only direct ionization and Ps formation, but also electronic excitation. The electronic excitation for the lowest-lying states in argon has been measured up to 30 eV to be

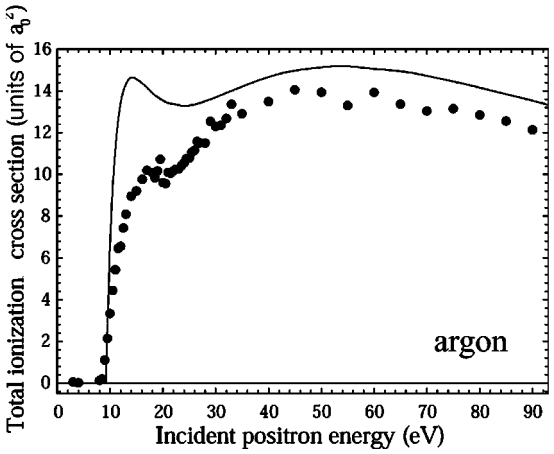

FIG. 8. Comparison of total ionization cross sections as a function of positron energy for argon (●) with the theoretical predictions (—) of Ref. [36] for the total inelastic cross section.

less than 1 a_0^2 [23], so while electronic excitation contributes to the higher values seen in the theory curves, it likely does so only slightly. For more details about the theory calculation, see Ref. [37].

V. SUMMARY AND CONCLUDING REMARKS

This paper presents absolute experimental measurements of the positronium formation and direct ionization cross sections in the noble gases, neon, argon, krypton, and xenon for positron energies from threshold to 90 eV. These data are compared to recent experimental measurements from Ref. [16] and theoretical calculations. Comparison of the present measurements of the cross sections for direct ionization and positronium formation with those of Ref. [16] show quantitative agreement for many features but some systematic differences.

Comparison of the *total* ionization measurements of Ref. [16] with those presented here showed good to excellent absolute agreement. In order to pursue further the differences between the measurements presented here and those in Ref. [16] for the direct ionization and positronium formation cross sections, another determination of the positronium formation and direct ionization cross sections was made, using the total ionization measurements of Ref. [16] and present measurements of the cross sections for the other process. In particular, the direct ionization cross sections (independently measured in the present work) and the total ionization cross sections of Ref. [16] yield another (independent) measure of the positronium formation cross sections. Similarly, the positronium formation cross sections (independently measured in the present work) and the total ionization cross sections of Ref. [16] yield another (independent) measure of the direct ionization cross sections.

This method of determining the positronium formation cross sections agrees well with the present measurements over most of the range of energies measured for argon, krypton, and xenon. This method of determining the direct ionization cross sections is also in agreement with the direct measurements of these cross sections presented here for the same atoms. The fact that these are two *independent* measurements of the cross sections, makes the results particularly significant. In the case of neon, some discrepancies remain in the measurements of both cross sections (i.e., $\sim \pm 15\%$), between the direct measurements and the indirect determination presented here and the measurements of Ref. [16].

Comparison of the direct ionization cross sections measured here and those of Ref. [16] indicated fairly good absolute agreement, with the former being somewhat larger than the latter from ~10% in argon to 30% in krypton.

As illustrated in Fig. 4, previous data for positronium formation cross sections in argon, krypton, and xenon [16] showed some evidence of a second peak in the cross section at energies 20–30 eV. These features have been attributed to phenomena such as the formation of excited-state positronium [16] and Ps formation by interaction with inner-shell electrons [11]. The two independent measures of the Ps formation cross sections presented here and illustrated in Fig. 4 show no evidence of these features. In the measurements presented here, there is a remaining feature in Xe, which is perhaps best described as a shoulder in the cross section (shown in the inset of Fig. 4). The onset of this feature is at ~15 eV, and is somewhat below the threshold for positronium formation from the 5*s* shell electrons, which is located at 16.7 eV in this target.

Comparison of the direct ionization cross section measurements with available theoretical predictions, as illustrated in Fig. 6, indicates reasonable absolute agreement over most of the range of energies studied. The exception is near threshold where the predicted cross sections of Refs. [27,28] in argon, krypton, and xenon are significantly larger than those observed.

Comparison of the measured positronium formation cross sections with theoretical predictions yields qualitative but not quantitative agreement. The shapes of the spectra agree reasonably well with the predictions of a recent distorted-wave Born approximation calculation [35] but there is a considerable discrepancy in the absolute values of the cross sections. The magnitudes of the cross sections agree better with the previous calculation of McAlinden and Walters [17] but not the dependence of the cross section on the energy. As mentioned above, we hope that the quality of the data now available and the importance of this problem in positron-atomic physics will stimulate further theoretical work.

ACKNOWLEDGMENTS

The authors wish to thank G. Laricchia, S. Gilmore, H. R. J. Walters, and R. I. Campeanu for providing numerical values of their data and calculations, and K. Bartschat and G. F. Gribakin for their unpublished calculations. The authors thank K. Bartschat, S. Buckman, R. I. Campeanu, S. Gilmore, G. F. Gribakin, G. Laricchia, and H. R. J. Walters for helpful conversations, and E. A. Jerzewski for his expert technical assistance. This work was supported by the National Science Foundation, Grant No. PHY 02-44653.

[1] T. C. Griffith and G. R. Heyland, Phys. Rep. **39C**, 169 (1978).
[2] W. E. Kauppila and T. S. Stein, Adv. At., Mol., Opt. Phys. **26**, 1 (1990).
[3] M. Charlton and J. Humberston, *Positron Physics* (Cambridge University Press, New York, 2001).
[4] *New Directions in Antimatter Chemistry and Physics*, edited by C. M. Surko and F. A. Gianturco (Kluwer Academic Publishers, Dordrecht, 2001).
[5] J. Moxom, P. Ashley, and G. Laricchia, Can. J. Phys. **74**, 367 (1996).
[6] F. M. Jacobsen, N. P. Frandsen, H. Knudsen, U. Mikkelsen, and D. M. Schrader, J. Phys. B **28**, 4691 (1995).
[7] V. Kara, K. Paludan, J. Moxom, P. Ashley, and G. Laricchia, J. Phys. B **30**, 3933 (1997).
[8] M. Charlton, G. Clark, T. C. Griffith, and G. R. Heyland, J. Phys. B **16**, L465 (1983).
[9] B. Jin, S. Miyamoto, O. Sueoka, and A. Hamada, Atomic Collisions Research in Japan **20**, 9 (1994).
[10] L. S. Fornari, L. M. Diana, and P. G. Coleman, Phys. Rev. Lett. **51**, 2276 (1983).
[11] T. S. Stein, M. Harte, M. Jiang, W. E. Kauppila, C. K. Kwan, H. Li, and S. Zhou, Nucl. Instrum. Methods Phys. Res. B **143**, 68 (1998).
[12] L. M. Diana, in *Proceedings of the 7th International Conference on Positron Annihilation*, edited by P. Jain, R. Singru, and K. Gopinathan (World Scientific, Singapore, 1985), p. 428.
[13] L. M. Diana *et al.*, in *Positron (Electron)–Gas Scattering*, edited by W. E. Kauppila, T. S. Stein, and J. Wadehra (World Scientific, Singapore, 1986), p. 296.
[14] L. Diana, P. G. Coleman, D. L. Brooks, and R. L. Chaplin, in *Atomic Physics with Positrons*, edited by J. W. Humberston and E. A. G. Armour (Plenum, New York, 1987), p. 55.
[15] L. M. Diana, D. L. Brooks, P. G. Coleman, R. L. Chaplin, and J. P. Howell, in *Positron Annihilation*, edited by L. Dorokins-Vanpraet, M. Dorokins, and D. Segers (World Scientific, Singapore, 1989), p. 311.
[16] G. Laricchia, P. V. Reeth, M. Szłuińska, and J. Moxom, J. Phys. B **35**, 2525 (2002).
[17] M. T. McAlinden and H. R. J. Walters, Hyperfine Interact. **73**, 65 (1992).
[18] S. J. Gilbert, C. Kurz, R. G. Greaves, and C. M. Surko, Appl. Phys. Lett. **70**, 1944 (1997).
[19] C. Kurz, S. J. Gilbert, R. G. Greaves, and C. M. Surko, Nucl. Instrum. Methods Phys. Res. B **143**, 188 (1998).
[20] S. J. Gilbert, R. G. Greaves, and C. M. Surko, Phys. Rev. Lett. **82**, 5032 (1999).
[21] J. P. Sullivan, S. J. Gilbert, J. P. Marler, R. G. Greaves, S. J. Buckman, and C. M. Surko, Phys. Rev. A **66**, 042708 (2002).
[22] J. P. Sullivan, S. J. Gilbert, and C. M. Surko, Phys. Rev. Lett. **86**, 1494 (2001).
[23] J. P. Sullivan, J. P. Marler, S. J. Gilbert, S. J. Buckman, and C. M. Surko, Phys. Rev. Lett. **87**, 073201 (2001).
[24] M. Szłuińska and G. Laricchia, Nucl. Instrum. Methods Phys. Res. B **221**, 107 (2004).
[25] In Ref. [11], Stein *et al.* identified this as a potential mechanism for structure in positronium formation cross sections.
[26] R. I. Campeanu, R. P. McEachran, and A. D. Stauffer, Nucl. Instrum. Methods Phys. Res. B **192**, 146 (2002).
[27] R. I. Campeanu, R. P. McEachran, and A. D. Stauffer, Can. J. Phys. **79**, 1231 (2001).
[28] R. I. Campeanu, L. Nagy, and A. D. Stauffer, Can. J. Phys. **81**, 919 (2003).
[29] K. Bartschat (unpublished).
[30] K. Bartschat and P. G. Burke, J. Phys. B **20**, 3191 (1987).
[31] K. Bartschat, Comput. Phys. Commun. **75**, 219 (1993).
[32] P. G. Burke and K. T. Taylor, J. Phys. B **8**, 2620 (1975).
[33] K. Bartschat and P. G. Burke, J. Phys. B **21**, 2969 (1988).
[34] K. Bartschat (unpublished).
[35] S. Gilmore, J. E. Blackwood, and H. R. J. Walters, Nucl. Instrum. Methods Phys. Res. B **221**, 129 (2004).
[36] G. F. Gribakin, in *Photonic, Electronic and Atomic Collisions*, edited by J. Burgdorfer, J. S. Cohen, S. Datz, and C. R. Vane (Rinton Press, Paramus, NJ, 2002), pp. 353–364; G. F. Gribakin (unpublished).
[37] G. F. Gribakin, Can. J. Phys. **74**, 449 (1996).